



# Composition dependence of phase transformation behavior and shape memory effect of Ti(Pt, Ir)

Y. Yamabe-Mitarai<sup>a,\*</sup>, T. Hara<sup>a</sup>, T. Kitashima<sup>a</sup>, S. Miura<sup>b</sup>, H. Hosoda<sup>c</sup>

<sup>a</sup> National Institute for Materials Science, 1-2-1 Sengen, Tsukuba, Ibaraki 305-0047, Japan

<sup>b</sup> Materials and Process Design, Division of Materials Science and Engineering, Hokkaido University, Sapporo 060-0813, Japan

<sup>c</sup> Precision and Intelligence Laboratory (P&I Lab), Tokyo Institute of Technology, Yokohama 226-8503, Japan

## ARTICLE INFO

### Article history:

Received 27 September 2011

Received in revised form 4 February 2012

Accepted 10 February 2012

Available online 5 March 2012

### Keywords:

High-temperature alloys

Intermetallics

Shape memory

SEM

X-ray diffraction

## ABSTRACT

The phase transformation and high-temperature shape memory effect of Ti(Pt, Ir) were investigated. First, the Ti-rich phase boundary of Ti(Pt, Ir) was investigated by phase composition analysis by secondary electron microscopy (SEM) using an electron probe X-ray micro analyzer (EPMA), X-ray diffraction analysis and transmission electron microscopy (TEM). Then, the three alloys Ti–35Pt–10Ir, Ti–22Pt–22Ir, and Ti–10Pt–32Ir (at%) close to the phase boundary but in the single phase of Ti(Pt, Ir) were prepared by the arc melting method. The shape memory effect and crystal structure were investigated by compression loading–unloading tests and high-temperature X-ray diffraction analysis, respectively.

© 2012 Elsevier B.V. All rights reserved.

## 1. Introduction

TiNi-based shape memory alloys are already in practical use, and the next stage is to develop high-temperature shape memory alloys (HTSMAs) for gas turbines, rocket engines, automotive engines, nuclear reactors, and so forth. This will require a higher martensitic transformation temperature. Several alloy systems have been proposed [1], including the addition of refractory metals such as Hf and Zr, and platinum group metals such as Pt and Pd, to TiNi. A significant body of data exists for Ti–Ni–Pd alloys, indicating acceptable work performance up to 35 at% Pd. The martensitic transformation temperature at 35 at% Pd is about 573 K, and it increases with higher Pd content [2]. However, at compositions above 35 at% Pd, recovery and recrystallization occur at operating temperatures in the range of 450–600 °C and irrecoverable strain becomes large [3], making it difficult to develop HTSMAs with Pd contents above about 35 at%. Therefore, research is now focusing on reducing irrecoverable strain in Ti–Ni–Pd alloys with Pd content of less than 35 at%. One advantage of Ti–Ni–Pt alloys with Pt content over 30 at% is that the martensitic transformation temperature is high above 773 K [4–6], but then deformation by creep becomes severe [7]. Similar to Ti–Ni–Pd, the desirable composition of Ti–Ni–Pt is considered to be below 30 at%.

Although Ti–Ni–Pd/Pt alloys still need to be improved, the addition of Pd and Pt is promising. We have focused on TiPt-based shape memory alloys [8–14]. In Ti–Pt alloys, the B2 parent phase (cubic structure) transforms to the B19 martensite phase (orthorhombic structure) and the transformation temperature of TiPt at equiatomic composition is about 1323 K [15]. Ir was chosen as a solid solution hardening element for TiPt, and the phase transformation and strain recovery were investigated for Ti<sub>50</sub>(Pt, Ir)<sub>50</sub> [8,9,11,13]. Transformation temperature increased by Ir addition and was found to be 1491 K in Ti–12.5Pt–37.5Ir [8,11]. The shape memory effect of Ti<sub>50</sub>(Pt, Ir)<sub>50</sub> was investigated by the thermal expansion test and compression test [11]. Strain recovery of 1.7% and recovery ratio of 57% were obtained in Ti–25Pt–25Ir after deformation at 1123 K followed by heat treatment above the transformation temperature, although recovery was not perfect. The change in crystal structure by addition of Ir was investigated by high-temperature X-ray diffractometry, and it was found that the structure changed from orthorhombic to almost tetragonal in the above composition range. An increase of tetragonality is thought to facilitate phase transformation, resulting in relatively good shape recovery [14]. However, although several alloy compositions have been tried, perfect recovery has not been achieved. Another question is how the B2 phase region extends in the Ti–Pt–Ir ternary system and how the addition of Ir changes the transformation temperature. In the Ir–Ti binary phase diagram, the transformation temperature is high for Ir-rich composition, but drastically decreases with increase of Ti content. When a large amount of Ir

\* Corresponding author. Tel.: +81 298 2525; fax: +81 298 2501.

E-mail address: [mitarai.yoko@nims.go.jp](mailto:mitarai.yoko@nims.go.jp) (Y. Yamabe-Mitarai).

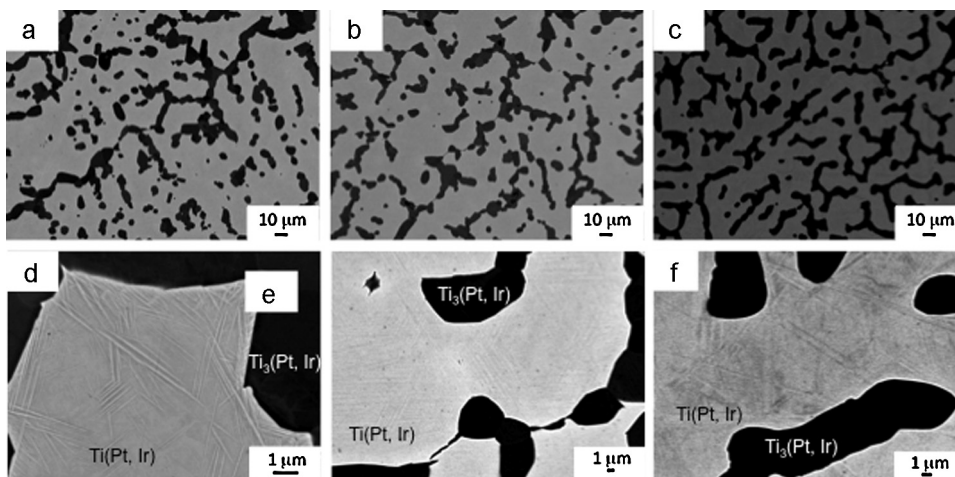


**Fig. 1.** Backscattered images of (a) Ti–27Pt–13Ir, (b) Ti–22Pt–22Ir, and (c) Ti–13Pt–27Ir alloys heat treated at 1523 K for 100 h followed by ice-water quenching. Enlarged backscattered images of (d) Ti–27Pt–13Ir, (e) Ti–22Pt–22Ir, and (f) Ti–13Pt–27Ir alloys heat treated in the same condition of (a–c).

is added to Ti–Pt, the transformation temperature in the Ti-rich region may be decreased drastically.

In this study, first the phase boundary of the B2 phase was investigated in the Ti-rich Ti–Pt–Ir ternary system. Based on the obtained phase boundary, several alloys with Ti-rich composition were prepared. The composition dependence of martensitic phase transformation temperature, crystal structure, and shape recovery was investigated.

## 2. Experimental procedure

Six kinds of 10-g alloy ingots with nominal composition of Ti–35Pt–10Ir, Ti–22Pt–22Ir, Ti–10Pt–32Ir, Ti–27Pt–13Ir, Ti–20Pt–20Ir and Ti–13Pt–27Ir (at%) were produced by the arc melting method. Ti–27Pt–13Ir, Ti–20Pt–20Ir and Ti–13Pt–27Ir are alloys with Ti content of 60 at%. These ingots were sealed in a silica tube with a small amount of Ar gas and heat treated for 168 h and/or 3 h depending on the alloy composition at 1523 K, a higher temperature than  $A_f$ . After heat treatment, the ingots were ice-water quenched.

Plate samples were sliced from the heat-treated ingot for microstructure observation. The sliced samples were embedded in resins and mechanically polished using sandpaper and diamond. The back-scattered images were taken at an accelerating voltage of 15 kV in a FE-SEM, JEOL 7001F. Phase composition was investigated in FE-SEM equipped with EPMA (JEOL JXA8900R). An accelerating voltage of 15 kV with a stabilized beam current of  $1 \times 10^{-7}$  A was used. Ti was analyzed using Ti K $\alpha$  S-ray lines with an LIF as the analyzing crystal, and Ir and Pt were analyzed using Ir M $\alpha$  and Pt M $\alpha$  X-ray lines with PETH as the analyzing crystal.

Sliced samples of 3 mm in diameter were cut from the heat-treated ingot for microstructure observation using TEM. The sliced samples were mechanically polished using sandpaper and ion milled, and the microstructure was observed at an accelerating voltage of 200 kV by TEM (Tecnai 20).

Small pieces measuring 2 mm  $\times$  2 mm  $\times$  0.8 mm were cut from button ingots and the phase transformation temperature was investigated by differential thermal analysis (DTA) between 473 and 1673 K at a heating and cooling rate of 0.17 K/s using a Shimadzu DTA-50.

Powder samples of micron order were prepared for Ti–35Pt–10Ir, Ti–22Pt–22Ir, and Ti–10Pt–32Ir by mechanically crushing heat-treated ingots for high-temperature X-ray diffraction analysis. The phase constituent was investigated at temperatures from room temperature to 1573 K using a Rigaku TTR-III high-temperature X-ray diffractometer equipped with Cu K $\alpha$  radiation. The powder samples were placed on an Al<sub>2</sub>O<sub>3</sub> plate in the Pt sample holder and heated in a vacuum furnace with a Pt heater. A Pt–Rh thermocouple was placed under the Pt holder to measure and control the temperature. The heating rate was 40 K/min and the samples were kept at the testing temperature for 5 min before X-ray analysis. The measurements from room temperature to 1573 K were conducted twice to remove plastic deformation obtained during preparation of powder samples by crushing.

Plate samples measuring 8 mm  $\times$  8 mm  $\times$  1 mm were used to investigate the structure of Ti–27Pt–13Ir, Ti–20Pt–20Ir, and Ti–13Pt–27Ir. The phase constituent was investigated at room temperature using a Rigaku 2500 equipped with Cu K $\alpha$  radiation.

Rectangular samples measuring 2.5 mm  $\times$  2.5 mm  $\times$  5 mm were cut from the ingots using an electrical discharge machine for the compression test. The loading–unloading compression test was carried out at an initial strain rate of

**Table 1**

Phase composition of Ti–Pt–Ir alloys analyzed by EPMA.

	Bright phase (at%)			Dark phase (at%)		
	Ti	Pt	Ir	Ti	Pt	Ir
Ti–27Pt–13Ir	57.1	29.1	13.8	69.0	22.6	8.4
Ti–20Pt–20Ir	58.2	21.6	20.2	68.7	19.3	12.0
Ti–13Pt–27Ir	59.8	13.9	26.3	69.7	15.3	15.0

$3 \times 10^{-4}$ /s at 1123 K using the Shimadzu AG–I test system. After the compression test, samples were heated at 1523 K for 1 h and the shape memory strain was measured by comparing the sample length before and after heat treatment.

## 3. Results and discussion

### 3.1. Phase boundary of the martensite phase

Microstructures of Ti–27Pt–13Ir, Ti–20Pt–20Ir, and Ti–13Pt–27Ir alloys observed after heat treatment at 1523 K for 168 h followed by ice-water quenching are shown in Fig. 1. Two phases, a dark phase and a bright phase, were observed in all three alloys as shown in Fig. 1a–c. In the enlarged microstructure in Fig. 1d–f, several straight lines similar to a twin structure were observed in the bright phase although the contrast is not clear. These straight lines suggest that the bright phase is the martensite phase. Phase compositions investigated by EPMA are summarized in Table 1. As expected from the microstructure in Fig. 1d–f, the composition of the bright phase is close to the martensite phase composition of Ti:60 and Pt+Ir:40. The composition of the dark phase was close to Ti:70 and Pt+Ir:30. According to the phase diagram of the Ti–Pt and Ti–Ir binary system [15], intermetallic compounds such as Ti<sub>3</sub>Pt and Ti<sub>3</sub>Ir appear in the composition range of 72–77 at% Ti for Ti–Pt and 73–75 at% Ti for Ti–Ir. X-ray diffraction analysis was conducted to confirm the phase structure for the heat-treated plate samples. In all the tested alloys, diffraction patterns from the martensite B19 phase were observed as shown in Fig. 2 and the bright phase can thus be identified as B19 phase. This indicates that the B2-parent phase at 1523 K was transformed to the B19-martensite phase during quenching. Peaks from the dark phase did not appear for some reason as shown in Fig. 2 despite the existence of several unknown peaks. In the A<sub>50</sub>B<sub>50</sub> compound, the tetragonal L1<sub>0</sub> is also a possible structure. For example, the L1<sub>0</sub> structure was found in IrTi at 1273 K where Ir is one of the platinum group metals the same as Pt [16]. Therefore,

Download English Version:

<https://daneshyari.com/en/article/1613831>

Download Persian Version:

<https://daneshyari.com/article/1613831>

[Daneshyari.com](https://daneshyari.com)